

\mathcal{X} -KD: General Experiential Knowledge Distillation for Large Language Models

Yuanyang Cai¹ Yuyu Yuan¹

Abstract

Knowledge Distillation (KD) for Large Language Models (LLMs) has become increasingly important as models grow in size and complexity. While existing distillation approaches focus on imitating teacher behavior, they often overlook the original learning environment that shaped the teacher’s knowledge. Inspired by the experiential learning theory and inverse reinforcement learning, we propose Experiential Knowledge Distillation (\mathcal{X} -KD), a novel and general framework that enables student models to learn in the teacher’s original learning environment. \mathcal{X} -KD adopts the Approximated Variational Reward Imitation Learning (AVRIL) framework to jointly model the teacher’s original reward function and perform policy distillation, encouraging consistency between the student policy and the original reward function. Our derivation demonstrates that \mathcal{X} -KD follows the supervised learning framework and applies to both sequence-level and divergence-based distillation methods, underlining the simplicity and flexibility of our approach. Empirical results show that \mathcal{X} -KD outperforms the generalized KD and MiniLLM baselines on abstractive summarization, machine translation, and arithmetic reasoning tasks. Additionally, \mathcal{X} -KD achieves better performance-diversity trade-off and data efficiency than baseline KD approaches.

1. Introduction

The Experiential Learning Theory (Kolb, 2014) proposes that experiencing the same environment as the original learner can provide the imitative learner with concrete experiences essential for effective learning. This theory is not only applicable to human learning but also to machine learning. In machine learning, research has shown that Inverse Reinforcement Learning (IRL) (Ng et al., 2000) generally has a better performance compared with Behavioral Cloning (BC) (Bain & Sammut, 1995) in expert imitation learning. A possible explanation is that in BC, the imitative learner (i.e., the training policy) simply imitates the behaviors of the original learner (i.e., the expert) while in IRL, the imitative

learner models the environment (i.e., the reward function) in which the original learner has learned and then places itself to learn in that environment.

The emergence of Large Language Models (LLMs) (Brown et al., 2020; Raffel et al., 2020; OpenAI, 2022; Achiam et al., 2023) results in the resurgence of knowledge distillation due to the limited energy and computational resources. Distillation is also a machine learning problem that involves imitative learners (i.e., students) learning from original learners (i.e., teachers). The distillation pipelines in the LLM era involve white-box distillation, where the teacher model is accessible, and black-box distillation, where the teacher model is inaccessible. Applying conventional white-box distillation approaches to LLMs suffers from distribution mismatch, lack of representation ability, and costly teacher-based data generation (Kim & Rush, 2016; Sanh et al., 2019). Wen et al. (2023) propose f -Divergence to address distribution mismatch brought by asymmetric distribution divergence. Liang et al. (2023) propose task-aware distillation, which improves the representation ability of distillation on specific tasks by filtering the useless information in hidden representation. Recently, GKD (Agarwal et al., 2024) leverages on-policy data and improved divergence to alleviate the issues. Black-box distillation is more relevant to prompt engineering and data augmentation, which considers not only the compression of the model but also the more nuanced process of knowledge elicitation and transfer (Xu et al., 2024).

In knowledge distillation, the teacher model acts as the original learner, while the student model acts as the imitative learner. Most existing distillation solutions for LLMs, such as use of on-policy data (Agarwal et al., 2024), improvements on divergence functions (Wen et al., 2023), and filter of hidden representation (Liang et al., 2023), focus mainly on better imitation of the teacher’s behavior without ascertaining the teacher’s original learning environment or putting the student to learn in the original environment. Likewise, black-box distillation approaches generally put the student model to learn in environments built upon fine-prompted teacher demonstrations or feedbacks (Xu et al., 2024), which do not directly maximize the reward of the original environment. None of these approaches put the student model into the teacher’s original learning environment to achieve experiential learning.

Recently, MiniLLM (Gu et al., 2024), the concurrent work with the GKD (Agarwal et al., 2024), proposes to use policy gradient to optimize the reverse KL distillation objective and proves its equivalence with the inverse reinforcement learning (IRL) framework, which considers the reward function of the teacher’s original learning environment and breaks through the scope of behavioral cloning. However, MiniLLM adopts the policy gradient method to maximize a reward function, which deviates from the supervised learning paradigm. On the other hand, MiniLLM relies on stabilizing techniques to address the training stability issue introduced by the policy gradient method. These features increase the complexity of integrating MiniLLM into existing LLM training frameworks and therefore may limit the application of MiniLLM’s training pipeline in engineering practice. Furthermore, MiniLLM cannot adapt to other divergence functions or sequence-level distillation for black-box models.

In this work, we propose Experiential Knowledge Distillation (\mathcal{X} -KD), a more general and flexible knowledge distillation approach that considers the reward function of the teacher’s original learning environment. We follow Approximated Variational Reward Imitation Learning (AVRIL) (Chan & van der Schaar, 2021), a Bayesian inverse reinforcement learning framework, to integrate experiential learning into sequence-level KD (Kim & Rush, 2016), supervised KD (forward-KL KD) (Hinton et al., 2015; Sanh et al., 2019), and GKD (Agarwal et al., 2024). Specifically, since AVRIL is able to jointly learn the reward function and the policy, we formulate the problem of jointly performing teacher reward learning and sequence-level KD as an AVRIL problem, and then generalize this formulation to forward-KL KD and GKD. Regarding flexibility, \mathcal{X} -KD applies to both sequence-level KD and divergence-based KD and does not limit the type of divergence functions. Regarding simplicity, the \mathcal{X} -KD objective consists of the corresponding original non-experiential KD objective and an experiential regularization term, which follows the supervised training paradigm.

Our work makes the following main contributions:

- We propose \mathcal{X} -KD, a novel knowledge distillation framework based on Bayesian inverse reinforcement learning that enables student models to learn in the teacher’s original learning environment, rather than just imitating teacher behavior.
- We demonstrate the flexibility and simplicity of \mathcal{X} -KD by integrating it with different knowledge distillation methods while maintaining the supervised learning framework.
- We empirically demonstrate that \mathcal{X} -KD outperforms baseline approaches across multiple NLG tasks while

achieving better performance-diversity trade-offs and improved data efficiency.

2. Preliminaries

2.1. Knowledge Distillation for LLMs

Knowledge distillation is generally a problem of training a small student model to transfer the knowledge of a large teacher model. Conventionally, there are two main types of distillation approaches for LLMs: sequence-level distillation (Kim & Rush, 2016) and supervised distillation (Hinton et al., 2015; Sanh et al., 2019). Sequence-level distillation maximizes the likelihood of sequences generated by the teacher. Given a prompt dataset \mathcal{D} , the teacher model π , and the student model π_θ , the sequence-level distillation objective can be denoted as Equation 1, which can be regarded as SFT on a teacher-generated dataset.

$$\max_{\theta} \sum_{\mathbf{x} \in \mathcal{D}} [\mathbb{E}_{\mathbf{y} \sim \pi(\cdot | \mathbf{x})} [\log \pi_\theta(\mathbf{y} | \mathbf{x})]] \quad (1)$$

Supervised distillation, on the other hand, minimizes the divergence of token-level distributions between the teacher and the student. Given a supervised fine-tuning (SFT) dataset \mathcal{D}_{SFT} , the training objective of supervised distillation can be denoted as Equation 2. Here, $D_{\text{KL}}(\pi || \pi_\theta)(\mathbf{y} | \mathbf{x})$ is the point-wise token-level Kullback-Leibler (KL) divergence with respect to the individual sample (\mathbf{x}, \mathbf{y}) , as shown in Equation 3, where $\mathbf{y}_{1:t} = (y_1, y_2, \dots, y_t)$ is the token sequence.

$$\min_{\theta} \mathbb{E}_{(\mathbf{x}, \mathbf{y}) \sim \mathcal{D}_{\text{SFT}}} [D_{\text{KL}}(\pi || \pi_\theta)(\mathbf{y} | \mathbf{x})] \quad (2)$$

$$D_{\text{KL}}(\pi || \pi_\theta)(\mathbf{y} | \mathbf{x}) = \frac{1}{|\mathbf{y}|} \sum_t D_{\text{KL}}[\pi(y_{t+1} | \mathbf{x}, \mathbf{y}_{1:t}) || \pi_\theta(y_{t+1} | \mathbf{x}, \mathbf{y}_{1:t})] \quad (3)$$

Recently, Agarwal et al. (2024) propose Generalized Knowledge Distillation (GKD) for LLMs, which leverages samples from student models for training and adopts a more generalized divergence function to avoid hallucination and low-quality generations. The GKD training objective can be denoted as Equation 4. Here, $D_\beta(\pi || B_\theta)(\mathbf{y} | \mathbf{x})$ denotes the point-wise token-level Jensen-Shannon (JS) divergence (Wen et al., 2023) with respect to the individual sample (\mathbf{x}, \mathbf{y}) , as illustrated in Equation 5.

$$\min_{\theta} \left[(1 - \alpha) \cdot \mathbb{E}_{(\mathbf{x}, \mathbf{y}) \sim \mathcal{D}_{\text{SFT}}} [D_\beta(\pi || \pi_\theta)(\mathbf{y} | \mathbf{x})] + \alpha \cdot \mathbb{E}_{\mathbf{x} \sim \mathcal{D}, \mathbf{y} \sim \pi_\theta(\mathbf{y} | \mathbf{x})} [D_\beta(\pi || \pi_\theta)(\mathbf{y} | \mathbf{x})] \right] \quad (4)$$

$$D_\beta(\pi || B_\theta)(\mathbf{y} | \mathbf{x}) = \frac{1}{|\mathbf{y}|} \sum_t D_\beta[\pi(y_{t+1} | \mathbf{x}, \mathbf{y}_{1:t}) || B_\theta(y_{t+1} | \mathbf{x}, \mathbf{y}_{1:t})] \quad (5)$$

2.2. MDP Formulation of NLG

The Natural Language Generation (NLG) task can be formulated as a Markov Decision Process (MDP) (Ranzato et al., 2016). At time step t , the state is the prompt along with the previously generated tokens, denoted as $s_t = (\mathbf{x}, \mathbf{y}_{1:t})$, and the action is the token to be generated $a_t = y_{t+1}$. The action space is the vocabulary \mathcal{V} containing all possible tokens. In text generation, the state transition is deterministic, so we do not consider the transition probability function. The reward of taking action y_{t+1} under state $(\mathbf{x}, \mathbf{y}_{1:t})$ is denoted as $R(\mathbf{x}, \mathbf{y}_{1:t+1})$, which attaches the action to the state for simplicity. The policy can be denoted as $\pi_\theta(y_{t+1}|\mathbf{x}, \mathbf{y}_{1:t})$, which is also the distribution of the language model parameterized by θ . For simplicity, we sometimes denote the policy as $\pi_\theta(\mathbf{y}|\mathbf{x}) = \prod_{t=1}^{|\mathbf{y}|-1} \pi_\theta(y_{t+1}|\mathbf{x}, \mathbf{y}_{1:t})$, where $|\mathbf{y}|$ is the length of sequence $|\mathbf{y}|$. Note that the accumulated product starts from $\pi_\theta(y_2|\mathbf{x}, \mathbf{y}_{1:1})$ instead of $\pi_\theta(y_1|\mathbf{x})$ since we assume that all sequences start with a special token denoting the start of the sequence.

2.3. Bayesian Inverse Reinforcement Learning

Inverse Reinforcement Learning (IRL) is the problem of extracting a reward function of an MDP given observed optimal behaviors (Ng et al., 2000). Bayesian Inverse Reinforcement Learning (BIRL) addresses the IRL problem with the Bayesian learning method. Given the behavioral data \mathcal{D} , BIRL formulates the reward distribution as a posterior distribution $p(R|\mathcal{D})$. The training objective is to approximate the posterior with a parameterized distribution $q_\phi(R)$, i.e., to minimize the KL divergence of $q_\phi(R)$ from $p(R|\mathcal{D})$, as shown in Equation 6. Since the posterior is intractable, an equivalent objective is adopted to maximize the Evidence Lower Bound (ELBO) of the KL divergence, as shown in Equation 7.

$$\min_{\phi} D_{\text{KL}}[q_\phi(R)||p(R|\mathcal{D})] \quad (6)$$

$$\max_{\phi} \mathbb{E}_{R \sim q_\phi(\cdot)} [\log p(\mathcal{D}|R)] - D_{\text{KL}}[q_\phi(R)||p(R)] \quad (7)$$

To practically optimize the ELBO training objective, (Chan & van der Schaar, 2021) propose Approximate Variational Reward Imitation Learning (AVRIL), which adopts approximated variational inference to jointly optimize a reward encoder and a Q-value decoder. The AVRIL training objective is as follows:

$$\max_{\phi, \theta} \sum_{(s, a, s', a') \in \mathcal{D}} \left[\log B_\theta(a|s) - D_{\text{KL}}[q_\phi(\cdot|s, a)||p(\cdot)] + \lambda \log q_\phi(\delta_\theta(s, a, s', a')|s, a) \right] \quad (8)$$

Here, $B_\theta(a|s)$ is the Boltzmann policy built upon the Q-

value decoder Q_θ parameterized by θ :

$$B_\theta(a|s) = \text{softmax}(\beta Q_\theta(s, a)) = \frac{\exp(\tau Q_\theta(s, a))}{\sum_{b \in \mathcal{A}} \exp(\tau Q_\theta(s, b))}$$

$q_\phi(\cdot|s, a)$ is the current reward distribution given the state s and the action a , $p(\cdot)$ is the prior reward distribution, and $\delta_\theta(s, a, s', a')$ is the TD error:

$$\delta_\theta(s, a, s', a') = Q_\theta(s, a) - \gamma Q_\theta(s', a')$$

The first term trains the Boltzmann policy to maximize the likelihood of the behaviors. The second term minimizes the KL divergence of the reward posterior from the prior. However, the likelihood is not conditioned on the reward, which is inconsistent with the ELBO training objective. The solution is the third term, which forces the TD error computed by the Q-value decoder to follow the reward distribution so that the behaviors are indirectly conditioned on the reward.

3. Experiential Knowledge Distillation

3.1. Original Reward Modeling

The objective of experiential learning for knowledge distillation is to enable the student model π_θ to learn in the original environment in which the teacher model π has learned. In other words, given the reward function R_π of the teacher's original environment, the objective of experiential learning is to encourage the student model to maximize the expected reward, as shown in Equation 9.

$$\max_{\theta} \mathbb{E}_{\mathbf{x} \sim \mathcal{D}, \mathbf{y} \sim \pi_\theta(\cdot|\mathbf{x})} [R_\pi(\mathbf{x}, \mathbf{y})] \quad (9)$$

However, the original reward function R_π is generally unknown. To estimate R_π , we assume that the original reward function follows a posterior distribution $R_\pi \sim p(R|\pi)$ and adopt a parameterized distribution $q_\phi(R)$ to approximate the posterior. The intuitive training objective of learning the original reward function is to minimize the KL divergence of $q_\phi(R)$ from $p(R|\pi)$, as shown in Equation 10. The equivalent objective is to maximize the ELBO of the KL divergence, as shown in Equation 11.

$$\min_{\phi} D_{\text{KL}}[q_\phi(R)||p(R|\pi)] \quad (10)$$

$$\max_{\phi} \mathbb{E}_{R \sim q_\phi(\cdot)} [\log p(\pi|R)] - D_{\text{KL}}[q_\phi(R)||p(R)] \quad (11)$$

We then approximate the ELBO objective using the AVRIL framework and obtain a practical Original Reward Modeling (ORM) training objective, as shown in Equation 12. The derivation is given in Appendix A.1. The ORM training objective is similar to the original AVRIL training objective (Equation 8) except that the state-action quadruple (s, a, s', a') is sampled from the teacher policy π instead of

the offline dataset \mathcal{D} , since we model the reward posterior $p(R|\pi)$ conditioning on the teacher policy.

$$\max_{\phi, \theta} \mathbb{E}_{(s, a, s', a') \sim \pi} \left[\begin{array}{l} \log \frac{\exp(\tau Q_\theta(s, a))}{\sum_{b \in \mathcal{A}} \exp(\tau Q_\theta(s, b))} \\ -D_{\text{KL}}[q_\phi(\cdot|s, a) || p(\cdot)] \\ + \lambda \log q_\phi(Q_\theta(s, a) - \gamma Q_\theta(s', a')) \end{array} \right] \quad (12)$$

Regarding the Natural Language Generation (NLG) process as a Markov Decision Process (MDP), given the prompt \mathbf{x} , at timestep t , the current state is the prompt along with the previously generated response, denoted by $s = (\mathbf{x}, \mathbf{y}_{1:t})$, the current action is the currently generated token, denoted by $a = y_{t+1}$, the next state is the prompt along with the currently generated response, denoted by $s' = (\mathbf{x}, \mathbf{y}_{1:t+1})$, and the next action is the next token to be generated, denoted by $a' = y_{t+2}$.

Therefore, given the prompt dataset \mathcal{D} and the teacher LLM policy π , we can materialize the ORM training objective (Equation 12) into the NLG setting by substituting the state-action quadruples with the specific states and actions during auto-regressive generation. The derivation is given in Appendix A.2. The loss function of the ORM training objective under the NLG setting is denoted as follows:

$$\mathcal{L}_{\text{orm}}(\phi, \theta) = - \sum_{\mathbf{x} \in \mathcal{D}} \mathbb{E}_{\mathbf{y} \sim \pi(\cdot|\mathbf{x})} [\mathcal{F}_{\text{avril}}(\mathbf{x}, \mathbf{y}; \phi, \theta)] \quad (13)$$

where $\mathcal{F}_{\text{avril}}$ denotes the AVRIL loss function with respect to the individual sample, as shown in Equation 14. B_θ is the Boltzmann policy for text generation, as shown in Equation 15, where $Q_\theta((\mathbf{x}, \mathbf{y}_{1:t}), y_{t+1})$ is the Q-value decoder denoting the state-action value of taking action y_{t+1} under state $\mathbf{y}_{1:t}$ and $q_\phi(\cdot|\mathbf{x}, \mathbf{y}_{1:t+1})$ is the distribution of the reward after taking action $a_t = y_{t+1}$ and transferring to state $s_{t+1} = \mathbf{y}_{1:t+1}$. $\delta_t(\theta)$ denotes the TD error at timestep t , i.e., the difference between the Q-value of the current action y_{t+1} and the discounted Q-value of the next action y_{t+2} , as shown in Equation 16.

$$\mathcal{F}_{\text{avril}}(\mathbf{x}, \mathbf{y}; \phi, \theta) = \sum_{t=1}^{|\mathbf{y}|} \left[\begin{array}{l} \log B_\theta(y_{t+1}|\mathbf{x}, \mathbf{y}_{1:t}) \\ -D_{\text{KL}}[q_\phi(\cdot|\mathbf{x}, \mathbf{y}_{1:t+1}) || p(\cdot)] \\ + \lambda \log q_\phi(\delta_t(\theta)|\mathbf{x}, \mathbf{y}_{1:t+1}) \end{array} \right] \quad (14)$$

$$B_\theta(y_{t+1}|\mathbf{x}, \mathbf{y}_{1:t}) = \frac{\exp(\tau Q_\theta((\mathbf{x}, \mathbf{y}_{1:t}), y_{t+1}))}{\sum_{y' \in \mathcal{V}} \exp(\tau Q_\theta((\mathbf{x}, \mathbf{y}_{1:t}), y'))} \quad (15)$$

$$\delta_t(\theta) = Q_\theta((\mathbf{x}, \mathbf{y}_{1:t}), y_{t+1}) - \gamma Q_\theta((\mathbf{x}, \mathbf{y}_{1:t+1}), y_{t+2}) \quad (16)$$

Note that we replace the expectation expression $\mathbb{E}_{\mathbf{x} \sim \mathcal{D}}$ by the summation expression $\sum_{\mathbf{x} \in \mathcal{D}}$, which does not affect the optimality of the training objective.

3.2. Sequence-Level X-KD

Regarding the Boltzmann policy B_θ as the student policy, the ORM objective (Equation 13) can be reformulated as the combination of a knowledge distillation objective and an experiential objective:

$$\mathcal{L}_{\text{orm}}(\phi, \theta) = \mathcal{L}_{\text{seq}}(\theta) + \mathcal{L}_{\text{ex}}(\phi, \theta) \quad (17)$$

Here, \mathcal{L}_{seq} is the sequence-level knowledge distillation (KD) objective (Kim & Rush, 2016) which distills the knowledge in the teacher policy π into the student policy B_θ :

$$\begin{aligned} \mathcal{L}_{\text{seq}}(\theta) &= - \sum_{\mathbf{x} \in \mathcal{D}} \mathbb{E}_{\mathbf{y} \sim \pi(\cdot|\mathbf{x})} [\log B_\theta(\mathbf{y}|\mathbf{x})] \\ &= - \sum_{\mathbf{x} \in \mathcal{D}} \mathbb{E}_{\mathbf{y} \sim \pi(\cdot|\mathbf{x})} \left[\sum_{t=1}^{|\mathbf{y}|} \log B_\theta(y_{t+1}|\mathbf{x}, \mathbf{y}_{1:t}) \right] \end{aligned} \quad (18)$$

\mathcal{L}_{ex} is the experiential objective ensuring the reward distribution to satisfy the prior distribution $p(R)$ and ensuring the student policy B_θ to satisfy the TD-error constraint under the reward distribution:

$$\mathcal{L}_{\text{ex}}(\phi, \theta) = \sum_{\mathbf{x} \in \mathcal{D}} \mathbb{E}_{\mathbf{y} \sim \pi(\cdot|\mathbf{x})} [\mathcal{F}_{\text{ex}}(\mathbf{x}, \mathbf{y}; \phi, \theta)] \quad (19)$$

where \mathcal{F}_{ex} is the sample-wise experiential objective:

$$\mathcal{F}_{\text{ex}}(\mathbf{x}, \mathbf{y}; \phi, \theta) = \sum_{t=1}^{|\mathbf{y}|} \left[\begin{array}{l} D_{\text{KL}}[q_\phi(\cdot|\mathbf{x}, \mathbf{y}_{1:t+1}) || p(\cdot)] \\ -\lambda \log q_\phi(\delta_t(\theta)|\mathbf{x}, \mathbf{y}_{1:t+1}) \end{array} \right] \quad (20)$$

Here, the hyperparameter λ is referred to as the experiential weight since it directly controls the degree of TD-error constraint.

The loss \mathcal{L}_{orm} can also be referred to as the sequence-level **Experiential Knowledge Distillation** (sequence-level X-KD) loss. By minimizing \mathcal{L}_{orm} , the student policy B_θ performs sequence-level knowledge distillation from the teacher policy π through the minimization of \mathcal{L}_{seq} , while staying consistent with the reward function of the teacher's original learning environment through the minimization of \mathcal{L}_{ex} , thus achieving experiential learning.

3.3. Supervised X-KD

The sequence-level KD objective \mathcal{L}_{seq} can further be written as Equation 21, where the first term in the square brackets is the KL divergence of the teacher policy π from the student policy B_θ . The derivation is given in Appendix A.3. Note that the second term is independent of the parameter θ , which can be ignored during optimization. In other words, minimizing the KL divergence is equivalent to minimizing \mathcal{L}_{seq} .

$$\mathcal{L}_{\text{seq}}(\theta) = \sum_{\mathbf{x} \in \mathcal{D}} \left[\begin{array}{l} D_{\text{KL}}[\pi(\cdot|\mathbf{x}) || B_\theta(\cdot|\mathbf{x})] \\ -\mathbb{E}_{\mathbf{y} \sim \pi(\cdot|\mathbf{x})} [\log \pi(\mathbf{y}|\mathbf{x})] \end{array} \right] \quad (21)$$

Therefore, we combine the KL divergence with the experiential objective to obtain the objective in Equation 22.

$$\begin{aligned}\mathcal{L}_{\text{xkd}}(\phi, \theta) &= \mathcal{L}_{\text{kd}}(\theta) + \mathcal{L}_{\text{ex}}(\phi, \theta) \\ &= \sum_{\mathbf{x} \in \mathcal{D}} D_{\text{KL}}[\pi(\cdot | \mathbf{x}) || B_{\theta}(\cdot | \mathbf{x})] + \mathcal{L}_{\text{ex}}(\phi, \theta)\end{aligned}\quad (22)$$

The loss \mathcal{L}_{xkd} is referred to as the supervised X-KD loss. By minimizing \mathcal{L}_{xkd} , the student policy B_{θ} performs supervised knowledge distillation from the teacher policy π through the minimization of \mathcal{L}_{kd} , while staying consistent with the reward function of the teacher's original learning environment through the minimization of \mathcal{L}_{ex} , thus achieving experiential learning.

3.4. Generalized X-KD

The sequence-level KD loss in Eq. 18 denotes a forward sequence-level KD objective, which encourages the student model to maximize the output probabilities of sentences generated by the teacher model. The corresponding reverse sequence-level KD objective is to encourage the student model to generate sentences that have higher probabilities under the teacher model, as shown in Eq. 23. A more general sequence-level KD objective can be denoted as the combination of the forward and the reverse objective, as shown in Eq. 24, where β is the hyperparameter balancing the two objectives.

$$\mathcal{L}_{\text{r-seq}}(\theta) = - \sum_{\mathbf{x} \in \mathcal{D}} \mathbb{E}_{\mathbf{y} \sim B_{\theta}(\cdot | \mathbf{x})} [\log \pi(\mathbf{y} | \mathbf{x})] \quad (23)$$

$$\mathcal{L}_{\text{g-seq}}(\theta) = \beta \cdot \mathcal{L}_{\text{seq}}(\theta) + (1 - \beta) \cdot \mathcal{L}_{\text{r-seq}}(\theta) \quad (24)$$

In supervised X-KD, we reformulate \mathcal{L}_{seq} as the combination of KL divergence and negative log-likelihood, as shown in Eq. 21. The derivation is given in Appendix A.3. The motivation is to obtain the conventional KL-based knowledge distillation loss \mathcal{L}_{kd} through the KL divergence. Similarly, we reformulate the general sequence-level KD loss $\mathcal{L}_{\text{g-seq}}$ as the combination of β -JS divergence and negative log-likelihood, as shown in Eq. 25.

$$\mathcal{L}_{\text{g-seq}}(\theta) = \sum_{\mathbf{x} \in \mathcal{D}} \begin{bmatrix} D_{\beta}[\pi(\cdot | \mathbf{x}) || B_{\theta}(\cdot | \mathbf{x})] \\ -\beta \mathbb{E}_{\mathbf{y} \sim \pi(\cdot | \mathbf{x})} [\log \pi(\mathbf{y} | \mathbf{x})] \\ -(1 - \beta) \mathbb{E}_{\mathbf{y} \sim B_{\theta}(\cdot | \mathbf{x})} [\log B_{\theta}(\mathbf{y} | \mathbf{x})] \end{bmatrix} \quad (25)$$

We then combine $\mathcal{L}_{\text{g-seq}}$ with the experiential loss \mathcal{L}_{ex} and remove unuseful terms to obtain the training objective in Eq. 26.

$$\begin{aligned}\mathcal{L}_{\text{g-xkd}}(\phi, \theta) &= \mathcal{L}_{\text{gkd}}(\theta) + \mathcal{L}_{\text{ex}}(\phi, \theta) \\ &= \sum_{\mathbf{x} \in \mathcal{D}} D_{\beta}[\pi(\cdot | \mathbf{x}) || B_{\theta}(\cdot | \mathbf{x})] + \mathcal{L}_{\text{ex}}(\phi, \theta)\end{aligned}\quad (26)$$

Algorithm 1 Generalized X-KD.

```

1: Input: prompt dataset  $\mathcal{D}$ , SFT dataset  $\mathcal{D}_{\text{SFT}}$ , teacher policy  $\pi$ , student policy  $p_{\theta}$ , reward distribution  $q_{\phi}$ 
2: Params: on-policy weight  $\alpha$ , experiential weight  $\lambda$ 
3: Output: new student policy  $p_{\theta}$ 
4: Fine-tune  $\pi$  and  $p_{\theta}$  with  $\mathcal{D}_{\text{SFT}}$ 
5: for  $k = 1, \dots, T_1$  do
6:   Sample  $u \sim \text{Uniform}(0, 1)$ 
7:   if  $u \leq \alpha$  then
8:     Sample  $\mathbf{x} \sim \mathcal{D}$ , and sample  $\mathbf{y} \sim p_{\theta}(\cdot | \mathbf{x})$ 
9:   else
10:    Sample  $(\mathbf{x}, \mathbf{y}) \sim \mathcal{D}_{\text{SFT}}$ 
11:   end if
12:    $\phi, \theta \leftarrow \nabla_{\phi, \theta} [D_{\beta}(\pi || p_{\theta})(\mathbf{y} | \mathbf{x}) + \mathcal{F}_{\text{ex}}(\mathbf{x}, \mathbf{y}; \phi, \theta)]$ 
13: end for
14: return  $p_{\theta}$ 

```

Algorithm 2 Black-box (sequence-level) X-KD.

```

1: Input: prompt dataset  $\mathcal{D}$ , black-box teacher policy  $\pi^*$ , student policy  $p_{\theta}$ , reward distribution  $q_{\phi}$ 
2: Params: experiential weight  $\lambda$ 
3: Output: new student policy  $p_{\theta}$ 
4: Fine-tune  $p_{\theta}$  with  $\mathcal{D}_{\text{SFT}}$ 
5: for  $k = 1, \dots, T_1$  do
6:   Sample  $u \sim \text{Uniform}(0, 1)$ 
7:   Sample  $\mathbf{x} \sim \mathcal{D}$ , and sample  $\mathbf{y} \sim \pi^*(\cdot | \mathbf{x})$ 
8:    $\phi, \theta \leftarrow \nabla_{\phi, \theta} [\log p_{\theta}(\mathbf{y} | \mathbf{x}) + \mathcal{F}_{\text{ex}}(\mathbf{x}, \mathbf{y}; \phi, \theta)]$ 
9: end for
10: return  $p_{\theta}$ 

```

Here, $\mathcal{L}_{\text{gkd}}(\theta)$ denotes the GKD loss, where the β -JS divergence is estimated using the mixture of on-policy and offline data, as shown in Eq. 27, with α denoting the ratio of on-policy data.

$$\mathcal{L}_{\text{gkd}}(\theta) = (1 - \alpha) \cdot \mathbb{E}_{(\mathbf{x}, \mathbf{y}) \in \mathcal{D}_{\text{SFT}}} [D_{\beta}(\pi || B_{\theta})(\mathbf{y} | \mathbf{x})] + \alpha \cdot \mathbb{E}_{\mathbf{x} \sim \mathcal{D}, \mathbf{y} \sim B_{\theta}(\cdot | \mathbf{x})} [D_{\beta}(\pi || B_{\theta})(\mathbf{y} | \mathbf{x})] \quad (27)$$

The loss $\mathcal{L}_{\text{g-xkd}}$ is referred to as the generalized X-KD loss. By minimizing $\mathcal{L}_{\text{g-xkd}}$, the student policy B_{θ} not only distills knowledge from the teacher policy π through the minimization of the GKD loss \mathcal{L}_{gkd} , but also stays consistent with the reward function of the teacher's original learning environment through the minimization of \mathcal{L}_{ex} , thus achieving experiential learning. Note that the loss $\mathcal{L}_{\text{g-xkd}}$ is based on the assumption that the loss \mathcal{L}_{seq} in Equation 17 can be replaced by any other sequence-level KD loss.

3.5. X-KD Pipelines

In the X-KD formulation, the student policy B_{θ} is denoted by the Q-value decoder Q_{θ} , and the computation of the X-KD loss depends on Q_{θ} . However, in language model

distillation, the student policy is generally initialized with a pre-trained language policy p_θ , without an explicit definition of the Q-value model. To compute the \mathcal{X} -KD objective through p_θ , we inversely formulate the Q-value decoder Q_θ as the log-softmax function of action probabilities, as shown in Equation 28, which is a non-strict inversion of the Boltzmann policy formulation.

$$Q_\theta((\mathbf{x}, \mathbf{y}_{1:t}), y_{t+1}) = \log \frac{\exp(\tau' \cdot p_\theta(y_{t+1} | \mathbf{x}, \mathbf{y}_{1:t}))}{\sum_{\mathbf{y}' \in \mathcal{V}} \exp(\tau' \cdot p_\theta(v | \mathbf{x}, \mathbf{y}_{1:t}))} \quad (28)$$

Given the teacher policy π and the student policy p_θ , the pipeline of generalized \mathcal{X} -KD is shown in Algorithm 1. Here, the computation of the sample-wise experiential objective $\mathcal{F}_{\text{ex}}(\mathbf{x}, \mathbf{y}; \phi, \theta)$ depends on the TD-error $\delta_t(\theta)$, as shown in Equation 20, where the experiential weight λ works. And the computation of the TD-error further depends on the Q-value function Q_θ , which is now substituted by Equation 28. The pipeline degenerates into supervised \mathcal{X} -KD when setting the on-policy weight α to 0, and degenerates into conventional non-experiential GKD when setting the experiential weight λ to 0.

The above pipeline only applies to white-box distillation where the output distribution of the teacher model is accessible. However, for some powerful language models, we only have access to their final output responses. Therefore, in addition to white-box \mathcal{X} -KD, we also directly leverage the sequence-level \mathcal{X} -KD objective (Equation 17) for black-box distillation, as shown in Algorithm 2. It is worth noting that Algorithm 2 also applies to white-box models as a sequence-level experiential distillation approach. The pipeline degenerates into conventional sequence-level distillation when setting the experiential weight λ to 0.

4. Experiment

Table 1. Overall results of \mathcal{X} -KD and baseline approaches on multiple NLG tasks with different model initializations.

	large \rightarrow small			large \rightarrow base		
	XSum	WMT	GSM	XSum	WMT	GSM
<i>Baselines</i>						
SFT	12.78	26.04	8.33	15.90	27.22	11.21
SeqKD	13.30	26.15	8.94	16.07	27.26	12.05
SKD	13.38	26.10	9.17	16.10	27.24	11.97
GKD	13.62	26.61	12.35	16.18	27.43	13.48
MiniLLM	13.69	26.65	12.50	16.15	27.54	13.41
<i>Ours</i>						
SeqXKD	13.36	26.23	9.32	16.09	27.28	12.42
S-XKD	13.45	26.63	10.53	16.12	27.44	12.50
G-XKD	13.81	26.73	12.35	16.24	27.61	13.63

4.1. Experiment Setup

Tasks and Datasets. We perform knowledge distillation on abstractive summarization, machine translation, and arithmetic reasoning tasks. For abstractive summarization, we use the XSum (Narayan et al., 2018) dataset containing news articles paired with single-sentence summaries. We evaluate the summarization performance on the validation set and report the ROUGE scores. For machine translation, we perform the English-to-German (en-de) translation task using the top 10k training data from the WMT14 (Bojar et al., 2014) de-en subset. We evaluate the translation performance on the validation set and report the BLEU scores. For arithmetic reasoning, we use the GSM8k (Cobbe et al., 2021) dataset containing grade school math word problems paired with detailed solutions. We use the same few-shot prompting as in GKD to improve the arithmetic reasoning performance. We evaluate the arithmetic reasoning performance on the test set and report the accuracy scores.

Model Initialization. For white-box distillation, we initialize the teacher and student with T5 model (Raffel et al., 2020) of different sizes. Specifically, we initialize the teacher models with T5-large (780M) and initialize the student models with T5-small (77M) and T5-base (250M). For black-box distillation, due to the expensive cost of invoking powerful black-box models, we employ Llama-2-7b as the black-box teacher model and adopt T5-large as the student model. For white-box teacher models and all student models, we perform supervised fine-tuning on specific tasks before knowledge distillation.

Baselines. We compare the \mathcal{X} -KD approaches with the baseline KD approaches that do not incorporate experiential learning. Specifically, for sequence-level or black-box distillation, we compare sequence-level \mathcal{X} -KD with the conventional sequence-level KD approach introduced in Kim & Rush (2016). For divergence-based distillation, we compare supervised \mathcal{X} -KD with the conventional supervised KD approach introduced in Hinton et al. (2015); Sanh et al. (2019), and compare generalized \mathcal{X} -KD with GKD (Agarwal et al., 2024). The hyperparameter configurations of various approaches are given in Appendix C.

Performance-Diversity. To explore the performance-diversity trade-off abilities of \mathcal{X} -KD, we adjust the sampling temperature to generate results with different diversities on the evaluation dataset. Specifically, we use 4 different sampling temperatures, which are 0.1, 0.3, 0.5, and 1.0. We then compute the SelfBLEU scores of different evaluation results to measure their diversities. A lower SelfBLEU score indicates more diverse outputs, therefore, we use 1 - SelfBLEU as the diversity score. Finally, we plot how performance scores vary with changes in the SelfBLEU score.

Data Efficiency Study. We perform data efficiency stud-

ies on all three NLG tasks to explore whether \mathcal{X} -KD can achieve comparable performance to baseline approaches with less distillation data. Specifically, we train baseline KD and \mathcal{X} -KD on 25%, 50%, 75%, and 100% of the training set. Here, we use T5-large as the teacher model and T5-small as the student model. The settings of training steps decrease proportionally with the training set.

Additional experiment results are included in Appendix B. More detailed experimental settings (e.g., hyperparameters) are included in Appendix C.

4.2. Abstractive Summarization

Our experiments on the XSum dataset demonstrate that \mathcal{X} -KD consistently outperforms the corresponding baseline approaches across both model size configurations. As shown in Table 1, under both model size settings, G-XKD outperforms the corresponding baselines GKD and MiniLLM, S-XKD outperforms the corresponding baseline SKD, and SeqXKD outperforms the corresponding baseline SeqKD.

The performance-diversity analysis in Figure 1a reveals that \mathcal{X} -KD maintains a better trade-off between summarization quality and diversity than GKD. Specifically, as diversity increases, the ROUGE-2 score of \mathcal{X} -KD decreases more slowly than that of GKD, indicating that experiential learning helps the student model learn more generalizable summarization strategies rather than simply mimicking teacher behavior.

The data efficiency results in Figure 1d demonstrate that generalized \mathcal{X} -KD achieves comparable performance to GKD while using 75% of the training data, suggesting that incorporating the teacher’s reward function helps capture fundamental summarization principles more efficiently.

4.3. Machine Translation

On the WMT14 English-to-German translation task, X-KD demonstrates robust improvements across different model sizes. As shown in Table 1, under both model size settings, \mathcal{X} -KD outperforms all corresponding baseline approaches.

Figure 1b demonstrates the performance-diversity trade-off on the WMT14 English-to-German task. Unlike the XSum task, not all distillation methods have monotonically decreasing performance-diversity curves on the WMT14 task. When the sampling temperature is 1.0 (the first point of each curve), the method with higher diversity achieves a higher BLEU score, indicating that assigning appropriate diversity to the decoding process is beneficial to the translation quality. When lowering the sampling temperature to 0.5 (the second point), the performance of GKD drops significantly, while the performance of experiential learning approaches (i.e., MiniLLM and X-GKD) improves, indicating that experiential learning facilitates the model to jointly achieve

translation quality and diversity. Here, G-XKD achieves a similar BLEU score to MiniLLM, but MiniLLM has better diversity. When the sampling temperature is 0.3 and 0.1 (the third and fourth points), the performance of the three methods is similar, but G-XKD has the best diversity, indicating that G-XKD can better maintain the translation quality at higher diversity.

The data efficiency analysis in Figure 1e mirrors the findings from the summarization task, i.e., \mathcal{X} -KD requires significantly less training data to achieve performance comparable to baselines trained on the full dataset. This consistent pattern across tasks suggests that experiential learning helps capture fundamental task principles rather than just surface-level patterns.

4.4. Arithmetic Reasoning

For arithmetic reasoning, we evaluate on the GSM8k dataset, which tests the models’ ability to solve grade school math word problems. As shown in Table 1, in both model settings, SeqXKD and S-XKD outperform SeqKD and SKD, respectively, which indicates that introducing experiential learning into sequence-level and forward-KL distillation improves the prediction accuracy. However, while G-XKD outperforms all baselines in the large \rightarrow base setting, it achieves identical performance to GKD and slightly underperforms MiniLLM in the large \rightarrow small setting. We attribute this to the small capacity of the student model, which results in a bottleneck in arithmetic reasoning ability.

Figure 1c demonstrates the performance-diversity trade-off on the GSM8k task. At a sampling temperature of 1.0, GKD demonstrates the most balanced performance-diversity characteristics. Shifting to temperatures of 0.5 and 0.3, G-XKD emerges as the method with the optimal performance-diversity trade-off. At a low temperature of 0.1, MiniLLM takes the lead in balancing performance and diversity. This series of results show that as the sampling temperature decreases and the diversity increases, experiential learning, especially the MiniLLM training objective, facilitates the model to maintain better arithmetic reasoning accuracies. However, at the temperature of 0.3, all three approaches achieve their best performances that are similar to each other, while G-XKD achieves the highest diversity. This observation suggests that G-XKD can achieve a good performance-diversity trade-off in arithmetic reasoning if the decoding temperature is tuned optimal.

The data efficiency results in Figure 1f show that when using 25% of the training data, G-XKD underperforms MiniLLM and GKD. However, when using 50% of the training data, G-XKD outperforms them and is even comparable to the performance achieved by these two approaches using 75% of the training data. When the training data ratio is 75% and 100%, the three methods achieve similar performance.

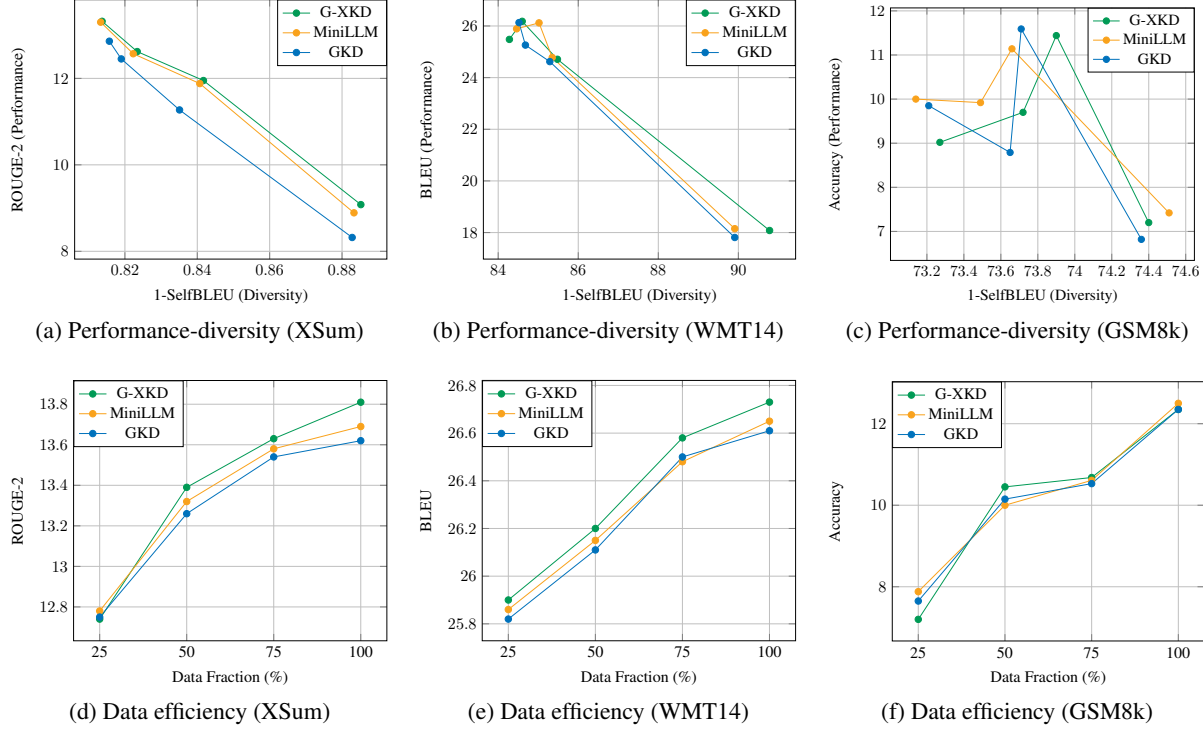


Figure 1. Performance-diversity and data efficiency curves of G-XKD, MiniLLM, and GKD.

Table 2. GPT-4 win rate evaluation of SeqXKD against SeqKD.

	Win	Tie	Lose
XSum	48.3%	8.7%	43.0%
WMT	43.8%	13.6%	42.6%
GSM	48.9%	2.8%	48.3%

4.5. Black-Box Distillation

We perform black-box distillation using SeqKD and SeqXKD, where Llama-2-7b is adopted as the teacher model and T5-large is adopted as the student model. We take the first 1000 data in each dataset and use Llama-2-7b to generate 10 answers for each source sentence in the dataset, thereby constructing an offline teacher behavior dataset $\mathcal{D}_{\text{teacher}}$. Then, in line 7 of Algorithm 2, instead of sampling the response from the online teacher model π^* , we directly use the response corresponding to x in $\mathcal{D}_{\text{teacher}}$. The distillation of black-box models does not use the ground truth in the dataset as supervision. Therefore, instead of evaluating the automatic metrics (ROUGE-2, BLEU, Accuracy), we employ GPT-4 to evaluate which response is better and report the win rate of our method SeqXKD against the baseline SeqKD.

Results in Table 2 show that SeqXKD outperforms SeqKD in win rate evaluation. In addition, the SeqXKD and SeqKD

experiments in Table 1 are also black-box KD using T5-large as the black-box teacher model, where the results of SeqXKD are also consistently higher than SeqKD. These findings indicate that SeqXKD with experiential learning provides better performance in black-box distillation.

5. Conclusion

We present \mathcal{X} -KD, a novel knowledge distillation framework for LLMs. By leveraging Bayesian inverse reinforcement learning, the framework enables student models to capture the underlying reward function of the teacher's learning environment. \mathcal{X} -KD's flexibility in integrating with different KD techniques and simplicity in maintaining a supervised learning paradigm highlight its potential for various applications. Experimental results show that \mathcal{X} -KD outperforms existing KD methods by delivering better performance, balancing performance and diversity, and improving data efficiency. However, we have to acknowledge that this paper has some limitations. Firstly, \mathcal{X} -KD's performance is sensitive to the tuning of the experiential weight, which increases the cost of hyperparameter tuning in practice. Secondly, the paper mainly focuses on the white-box setting and pays less attention to the black-box setting claimed applicable. We will conduct a more systematic study with \mathcal{X} -KD in black-box distillation in the future.

Impact Statement

This paper presents work whose goal is to advance the field of Machine Learning. There are many potential societal consequences of our work, none which we feel must be specifically highlighted here.

References

Achiam, J., Adler, S., Agarwal, S., Ahmad, L., Akkaya, I., Aleman, F. L., Almeida, D., Altenschmidt, J., Altman, S., Anadkat, S., et al. Gpt-4 technical report. *arXiv preprint arXiv:2303.08774*, 2023.

Agarwal, R., Vieillard, N., Zhou, Y., Stanczyk, P., Garea, S. R., Geist, M., and Bachem, O. On-policy distillation of language models: Learning from self-generated mistakes. In *The Twelfth International Conference on Learning Representations*, 2024.

Bain, M. and Sammut, C. A framework for behavioural cloning. In *Machine Intelligence 15*, pp. 103–129, 1995.

Bojar, O., Buck, C., Federmann, C., Haddow, B., Koehn, P., Leveling, J., Monz, C., Pecina, P., Post, M., Saint-Amand, H., et al. Findings of the 2014 workshop on statistical machine translation. In *Proceedings of the ninth workshop on statistical machine translation*, pp. 12–58, 2014.

Brown, T., Mann, B., Ryder, N., Subbiah, M., Kaplan, J. D., Dhariwal, P., Neelakantan, A., Shyam, P., Sastry, G., Askell, A., et al. Language models are few-shot learners. *Advances in neural information processing systems*, 33: 1877–1901, 2020.

Chan, A. J. and van der Schaar, M. Scalable Bayesian inverse reinforcement learning. In *International Conference on Learning Representations*, 2021. URL <https://openreview.net/forum?id=4qR3coiNaIV>.

Cobbe, K., Kosaraju, V., Bavarian, M., Chen, M., Jun, H., Kaiser, L., Plappert, M., Tworek, J., Hilton, J., Nakano, R., et al. Training verifiers to solve math word problems. *arXiv preprint arXiv:2110.14168*, 2021.

Dettmers, T., Pagnoni, A., Holtzman, A., and Zettlemoyer, L. Qlora: efficient finetuning of quantized llms (2023). *arXiv preprint arXiv:2305.14314*, 52:3982–3992, 2023.

Gu, Y., Dong, L., Wei, F., and Huang, M. Minilm: Knowledge distillation of large language models. In *The Twelfth International Conference on Learning Representations*, 2024.

Hinton, G., Vinyals, O., and Dean, J. Distilling the knowledge in a neural network. *arXiv preprint arXiv:1503.02531*, 2015.

Hu, E. J., Shen, Y., Wallis, P., Allen-Zhu, Z., Li, Y., Wang, S., Wang, L., and Chen, W. Lora: Low-rank adaptation of large language models. *arXiv preprint arXiv:2106.09685*, 2021.

Kim, Y. and Rush, A. M. Sequence-level knowledge distillation. *arXiv preprint arXiv:1606.07947*, 2016.

Kolb, D. A. *Experiential learning: Experience as the source of learning and development*. FT press, 2014.

Liang, C., Zuo, S., Zhang, Q., He, P., Chen, W., and Zhao, T. Less is more: Task-aware layer-wise distillation for language model compression. In *International Conference on Machine Learning*, pp. 20852–20867. PMLR, 2023.

Narayan, S., Cohen, S. B., and Lapata, M. Don’t give me the details, just the summary! topic-aware convolutional neural networks for extreme summarization. *arXiv preprint arXiv:1808.08745*, 2018.

Ng, A. Y., Russell, S., et al. Algorithms for inverse reinforcement learning. In *Icml*, volume 1, pp. 2, 2000.

OpenAI. Introducing chatgpt. <https://openai.com/index/chatgpt/>, 2022.

Raffel, C., Shazeer, N., Roberts, A., Lee, K., Narang, S., Matena, M., Zhou, Y., Li, W., and Liu, P. J. Exploring the limits of transfer learning with a unified text-to-text transformer. *Journal of machine learning research*, 21 (140):1–67, 2020.

Ranzato, M., Chopra, S., Auli, M., and Zaremba, W. Sequence level training with recurrent neural networks. In *4th International Conference on Learning Representations, ICLR 2016*, 2016.

Sanh, V., Debut, L., Chaumond, J., and Wolf, T. Distilbert, a distilled version of bert: smaller, faster, cheaper and lighter. *arXiv preprint arXiv:1910.01108*, 2019.

Sutton, R. S. and Barto, A. G. *Reinforcement learning: An introduction*. MIT press, 2018.

Wen, Y., Li, Z., Du, W., and Mou, L. f-divergence minimization for sequence-level knowledge distillation. *arXiv preprint arXiv:2307.15190*, 2023.

Xu, X., Li, M., Tao, C., Shen, T., Cheng, R., Li, J., Xu, C., Tao, D., and Zhou, T. A survey on knowledge distillation of large language models. *arXiv preprint arXiv:2402.13116*, 2024.

Yim, J., Joo, D., Bae, J., and Kim, J. A gift from knowledge distillation: Fast optimization, network minimization and transfer learning. In *Proceedings of the IEEE conference on computer vision and pattern recognition*, pp. 4133–4141, 2017.

A. Derivations

A.1. Original Reward Modeling

The original reward modeling objective is to learn the reward function based on which the teacher policy π is trained. In Section 3.1, we intuitively apply the AVRIL framework to the original reward modeling ELBO objective in Equation 11 and obtain the training objective in Equation 12. Here, we give the detailed derivation.

Given the ELBO objective:

$$\max_{\phi} \mathbb{E}_{R \sim q_{\phi}(\cdot)} [\log p(\pi|R)] - D_{\text{KL}}[q_{\phi}(R) || p(R)] \quad (29)$$

The likelihood $p(\pi|R)$ denotes the probability of obtaining policy π under the reward function R . Let π_R be the optimal policy under reward R , $\mathcal{D}_{\pi} \sim \pi(\cdot)$ is the behavioral data sampled from policy π . Then, $p(\pi|R)$ can be regarded as $p(\mathcal{D}_{\pi}|\pi_R)$, which means the probability of behavior \mathcal{D}_{π} under policy π_R and can be further denoted as Equation 30, where $\pi_R(a|s)$ is the probability of action a given state s under policy π_R .

$$p(\pi|R) = p(\mathcal{D}_{\pi}|\pi_R) = \mathbb{E}_{(s,a) \sim \pi} [\pi_R(a|s)] \quad (30)$$

The policy π_R can be formulated as a Boltzmann policy, as shown in Equation 31, where $Q_R^{\pi_R}$ is the state-action value function under reward function R and policy π_R .

$$\pi_R(a|s) = \frac{\exp(\tau Q_R^{\pi_R}(s, a))}{\sum_{b \in \mathcal{A}} \exp(\tau Q_R^{\pi_R}(s, b))} \quad (31)$$

By substituting Equation 31 into the ELBO objective, we obtain an equivalent objective, as shown in Equation 32. Note that here we move the log into the expectation over $(s, a) \sim \pi$, which does not affect the optimality of the training objective.

$$\max_{\phi} \mathbb{E}_{R \sim q_{\phi}} \left[\log \mathbb{E}_{(s,a) \sim \pi} \left[\frac{\exp(\tau Q_R^{\pi_R}(s, a))}{\sum_{b \in \mathcal{A}} \exp(\tau Q_R^{\pi_R}(s, b))} \right] - D_{\text{KL}}[q_{\phi}(R) || p(R)] \right] \quad (32)$$

To evaluate $Q_R^{\pi_R}(s, a)$, we use a neural network Q_{θ} parameterized by θ to approximate the state-action value:

$$Q_R^{\pi_R}(s, a) \approx Q_{\theta}(s, a) \quad (33)$$

By directly replacing $Q_R^{\pi_R}$ with $Q_{\theta}(s, a)$ in Equation 32 and considering the optimization of the newly introduced parameter θ , we obtain a new training objective:

$$\max_{\phi, \theta} \mathbb{E}_{R \sim q_{\phi}} \left[\log \mathbb{E}_{(s,a) \sim \pi} \left[\frac{\exp(\tau Q_{\theta}(s, a))}{\sum_{b \in \mathcal{A}} \exp(\tau Q_{\theta}(s, b))} \right] - D_{\text{KL}}[q_{\phi}(R) || p(R)] \right] \quad (34)$$

However, this objective is not equivalent to the original ELBO objective in Equation 29. The original objective (Equation 32) maximizes the parameter ϕ based on the strict state-action value function $Q_R^{\pi_R}$, while Equation 34 maximizes the approximated state-action value function Q_{θ} . This sounds feasible, but there is no objective to draw Q_{θ} close to $Q_R^{\pi_R}$. Therefore, Q_{θ} may become completely different from $Q_R^{\pi_R}$, and thus the objective in Equation 34 is completely different from that in Equation 32.

To address the problem, the AVRIL framework introduces a constraint term. According to the Bellman equation (Sutton & Barto, 2018), the relationship between reward function R and the state-action value function $Q_R^{\pi_R}$ under this reward satisfies the following equation:

$$R(s, a) = \mathbb{E}_{(s',a') \sim \pi_R} [Q_R^{\pi_R}(s, a) - \gamma Q_R^{\pi_R}(s', a')] \quad (35)$$

In other words, for the parameterized state-action value function Q_{θ} , if Q_{θ} is trained under the reward function R , then Q_{θ} must satisfy Equation 36 for any (s, a) .

$$\mathbb{E}_{(s',a') \sim \pi_R} [Q_{\theta}(s, a) - \gamma Q_{\theta}(s', a')] = R(s, a) \quad (36)$$

Therefore, AVRIL adds a constraint to the training objective in Equation 34 and obtains the training objective in Equation 37.

$$\max_{\phi, \theta} \mathbb{E}_{R \sim q_{\phi}} \left[\mathbb{E}_{(s,a) \sim \pi} \left[\log \frac{\exp(\tau Q_{\theta}(s, a))}{\sum_{b \in \mathcal{A}} \exp(\tau Q_{\theta}(s, b))} \right] - D_{\text{KL}}[q_{\phi}(R) || p(R)] \right]$$

subject to

$$\mathbb{E}_{(s,a,s',a') \sim \pi} [-\log q_{\phi}(Q_{\theta}(s, a) - \gamma Q_{\theta}(s', a'))] < \epsilon \quad (37)$$

Rewriting Equation 37 as a Lagrangian under the KKT conditions, and given complimentary slackness, a practical objective function can be obtained, as shown in Equation 38. Note that here we remove the expectation over $R \sim q_{\phi}$ for approximation, which is also performed in AVRIL (Chan & van der Schaar, 2021). Equation 38 is exactly the ORM training objective in Equation 12.

$$\max_{\phi, \theta} \mathbb{E}_{(s,a,s',a') \sim \pi} \left[\frac{\log \exp(\tau Q_{\theta}(s, a))}{\sum_{b \in \mathcal{A}} \exp(\tau Q_{\theta}(s, b))} - D_{\text{KL}}[q_{\phi}(\cdot|s, a) || p(\cdot)] + \lambda \log q_{\phi}(Q_{\theta}(s, a) - \gamma Q_{\theta}(s', a')) \right] \quad (38)$$

A.2. ORM in NLG Setting

Determining the meaning of the state and action quadruple (s, a, s', s') in Equation 12 (i.e., 38) is the first step in applying the ORM training objective to a specific problem. As clarified in Section 3.1, in the NLG setting, given the prompt \mathbf{x} , at timestep t , the current state is $s = (\mathbf{x}, \mathbf{y}_{1:t})$, the current

action is $a = y_{t+1}$, the next state is $s' = (\mathbf{x}, \mathbf{y}_{1:t+1})$, and the next action is $a' = y_{t+2}$. Therefore, the sampling of a from policy π given the state s , which is originally denoted as $a \sim \pi(\cdot|s)$, is now denoted as $y_{t+1} \sim \pi(\cdot|\mathbf{x}, \mathbf{y}_{1:t})$, which is the auto-regressive generation given π as the language model. Furthermore, the expectation over state-action quadruples $\mathbb{E}_{(s, a, s', a') \sim \pi}[f(s, a, s', a')]$ is now denoted as:

$$\mathbb{E}_{\mathbf{x} \sim \mathcal{D}} \mathbb{E}_{\mathbf{y} \sim \pi(\cdot|\mathbf{x})} \sum_{t=1}^{|\mathbf{y}|} f\left(\overbrace{(\mathbf{x}, \mathbf{y}_{1:t})}^s, \underbrace{y_{t+1}}_a, \overbrace{(\mathbf{x}, \mathbf{y}_{1:t+1})}^{s'}, \underbrace{y_{t+2}}_{a'}\right) \quad (39)$$

where \mathcal{D} is the prompt dataset denoting the initial state distribution.

Applying the format in Equation 39 to the ORM training objective in Equation 38, we obtain the ORM training objective in the NLG setting, as shown in Equation 40, which is exactly the objective in Equation 13.

$$-\sum_{\mathbf{x} \in \mathcal{D}} \mathbb{E}_{\mathbf{y} \sim \pi(\cdot|\mathbf{x})} \left[\sum_{t=1}^{|\mathbf{y}|} \left[\log \frac{\exp(\tau Q_\theta((\mathbf{x}, \mathbf{y}_{1:t}), y_{t+1}))}{\sum_{y' \in \mathcal{V}} \exp(\tau Q_\theta((\mathbf{x}, \mathbf{y}_{1:t}), y'))} \right] - D_{\text{KL}}[q_\phi(\cdot|\mathbf{x}, \mathbf{y}_{1:t+1})||p(\cdot)] + \lambda \log q_\phi(\delta_t(\theta)|\mathbf{x}, \mathbf{y}_{1:t+1}) \right] \quad (40)$$

A.3. Sequence-Level KD Loss Reformulation

In Section 3.3, we reformulate the sequence-level loss function as Equation 21, which separates the forward-KL $D_{\text{KL}}(\pi(\cdot|\mathbf{x})||B_\theta(\cdot|\mathbf{x}))$ from the sequence-level loss. The detailed derivation is as follows:

$$\begin{aligned} \mathcal{L}_{\text{seq}}(\theta) &= -\sum_{\mathbf{x} \in \mathcal{D}} \mathbb{E}_{\mathbf{y} \sim \pi(\cdot|\mathbf{x})} [\log B_\theta(\mathbf{y}|\mathbf{x})] \\ &= -\sum_{\mathbf{x} \in \mathcal{D}} \mathbb{E}_{\mathbf{y} \sim \pi(\cdot|\mathbf{x})} \left[\log B_\theta(\mathbf{y}|\mathbf{x}) - \log \pi(\mathbf{y}|\mathbf{x}) + \log \pi(\mathbf{y}|\mathbf{x}) \right] \\ &= -\sum_{\mathbf{x} \in \mathcal{D}} \mathbb{E}_{\mathbf{y} \sim \pi(\cdot|\mathbf{x})} \left[\log \frac{B_\theta(\mathbf{y}|\mathbf{x})}{\pi(\mathbf{y}|\mathbf{x})} + \log \pi(\mathbf{y}|\mathbf{x}) \right] \\ &= -\sum_{\mathbf{x} \in \mathcal{D}} \mathbb{E}_{\mathbf{y} \sim \pi(\cdot|\mathbf{x})} \left[-\log \frac{\pi(\mathbf{y}|\mathbf{x})}{B_\theta(\mathbf{y}|\mathbf{x})} + \log \pi(\mathbf{y}|\mathbf{x}) \right] \\ &= \sum_{\mathbf{x} \in \mathcal{D}} \mathbb{E}_{\mathbf{y} \sim \pi(\cdot|\mathbf{x})} \left[\log \frac{\pi(\mathbf{y}|\mathbf{x})}{B_\theta(\mathbf{y}|\mathbf{x})} - \log \pi(\mathbf{y}|\mathbf{x}) \right] \\ &= \sum_{\mathbf{x} \in \mathcal{D}} \left[D_{\text{KL}}[\pi(\cdot|\mathbf{x})||B_\theta(\cdot|\mathbf{x})] - \mathbb{E}_{\mathbf{y} \sim \pi(\cdot|\mathbf{x})} [\log \pi(\mathbf{y}|\mathbf{x})] \right] \end{aligned}$$

In Section 3.4, we reformulate the combination of forward and reverse sequence-level loss functions (Equation 24) as

Equation 25, which separates the Jensen-Shannon divergence $D_\beta(\pi(\cdot|\mathbf{x})||B_\theta(\cdot|\mathbf{x}))$ from the sequence-level loss. The detailed derivation is as follows:

$$\begin{aligned} \mathcal{L}_{\text{g-seq}}(\theta) &= \beta \cdot \mathcal{L}_{\text{seq}}(\theta) + (1 - \beta) \cdot \mathcal{L}_{\text{r-seq}}(\theta) \\ &= -\beta \cdot \sum_{\mathbf{x} \in \mathcal{D}} \mathbb{E}_{\mathbf{y} \sim \pi(\cdot|\mathbf{x})} [\log B_\theta(\mathbf{y}|\mathbf{x})] \\ &\quad - (1 - \beta) \cdot \sum_{\mathbf{x} \in \mathcal{D}} \mathbb{E}_{\mathbf{y} \sim B_\theta(\cdot|\mathbf{x})} [\log \pi(\mathbf{y}|\mathbf{x})] \\ &= \beta \cdot \sum_{\mathbf{x} \in \mathcal{D}} \left[D_{\text{KL}}[\pi(\cdot|\mathbf{x})||B_\theta(\cdot|\mathbf{x})] - \mathbb{E}_{\mathbf{y} \sim \pi(\cdot|\mathbf{x})} [\log \pi(\mathbf{y}|\mathbf{x})] \right] \\ &\quad - (1 - \beta) \cdot \sum_{\mathbf{x} \in \mathcal{D}} \mathbb{E}_{\mathbf{y} \sim B_\theta(\cdot|\mathbf{x})} \left[\log \frac{\pi(\mathbf{y}|\mathbf{x})}{B_\theta(\mathbf{y}|\mathbf{x})} + \log B_\theta(\mathbf{y}|\mathbf{x}) \right] \\ &= \beta \cdot \sum_{\mathbf{x} \in \mathcal{D}} \left[D_{\text{KL}}[\pi(\cdot|\mathbf{x})||B_\theta(\cdot|\mathbf{x})] - \mathbb{E}_{\mathbf{y} \sim \pi(\cdot|\mathbf{x})} [\log \pi(\mathbf{y}|\mathbf{x})] \right] \\ &\quad + (1 - \beta) \cdot \sum_{\mathbf{x} \in \mathcal{D}} \left[D_{\text{KL}}[B_\theta(\cdot|\mathbf{x})||\pi(\cdot|\mathbf{x})] - \mathbb{E}_{\mathbf{y} \sim B_\theta(\cdot|\mathbf{x})} [\log B_\theta(\mathbf{y}|\mathbf{x})] \right] \\ &= \sum_{\mathbf{x} \in \mathcal{D}} \left[\begin{array}{l} \beta \cdot D_{\text{KL}}[\pi(\cdot|\mathbf{x})||B_\theta(\cdot|\mathbf{x})] \\ + (1 - \beta) \cdot D_{\text{KL}}[B_\theta(\cdot|\mathbf{x})||\pi(\cdot|\mathbf{x})] \\ - \beta \mathbb{E}_{\mathbf{y} \sim \pi(\cdot|\mathbf{x})} [\log \pi(\mathbf{y}|\mathbf{x})] \\ - (1 - \beta) \mathbb{E}_{\mathbf{y} \sim B_\theta(\cdot|\mathbf{x})} [\log B_\theta(\mathbf{y}|\mathbf{x})] \end{array} \right] \\ &= \sum_{\mathbf{x} \in \mathcal{D}} \left[\begin{array}{l} D_\beta[\pi(\cdot|\mathbf{x})||B_\theta(\cdot|\mathbf{x})] \\ - \beta \mathbb{E}_{\mathbf{y} \sim \pi(\cdot|\mathbf{x})} [\log \pi(\mathbf{y}|\mathbf{x})] \\ - (1 - \beta) \mathbb{E}_{\mathbf{y} \sim B_\theta(\cdot|\mathbf{x})} [\log B_\theta(\mathbf{y}|\mathbf{x})] \end{array} \right] \end{aligned}$$

The red terms above are ignored during optimization. Specifically, $\mathbb{E}_{\mathbf{y} \sim \pi(\cdot|\mathbf{x})} [\log \pi(\mathbf{y}|\mathbf{x})]$ is not relevant to the parameter θ and is therefore ignored in optimization. On the other hand, maximizing $\mathbb{E}_{\mathbf{y} \sim B_\theta(\cdot|\mathbf{x})} [\log B_\theta(\mathbf{y}|\mathbf{x})]$ literally means maximizing the probability of sentences generated by the B_θ strategy under B_θ , which is redundant and therefore also ignored. Therefore, minimizing $\mathcal{L}_{\text{seq}}(\theta)$ is equivalent to minimizing the forward KL divergence between π and B_θ , and minimizing $\mathcal{L}_{\text{g-seq}}(\theta)$ is equivalent to minimizing the Jensen-Shannon divergence between π and B_θ .

B. Additional Experiments

B.1. Scalability Study

To investigate the scalability of X-KD, we examine how variations in model size, for both teacher and student architectures, influence distillation performance. While our primary analysis employs T5-small and T5-base as student models with T5-large as the teacher model, we conduct additional experiments across more detailed configurations. In one set of experiments, we maintain T5-small as the student model while systematically employing larger teacher

Table 3. Self-distillation performances on three tasks.

	XSum	WMT	GSM8k
GKD	18.33	27.48	23.33
G-XKD	18.46	27.67	23.48

models: T5-base, T5-large, and T5-xl. Conversely, we fix T5-xl as the teacher model and evaluate the performance using progressively larger student models: T5-small, T5-base, and T5-large. We implement GKD and G-XKD distillation approaches on the XSum dataset across these configurations, with results presented in Figure 2. The empirical evidence demonstrates that G-XKD consistently achieves superior performance compared to GKD, regardless of the size increases in either the teacher or student model.

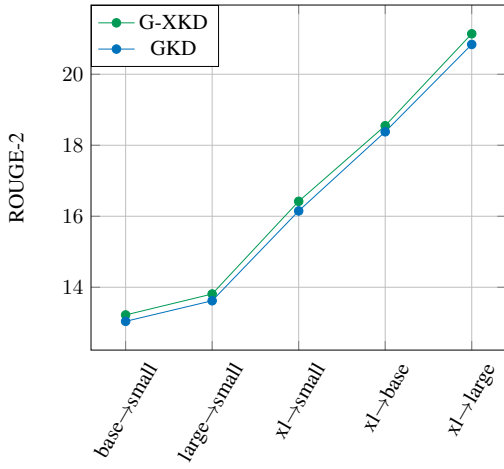


Figure 2. Scalability of G-XKD and GKD.

B.2. Self-Distillation

Self-distillation (Yim et al., 2017) involves distilling knowledge from a teacher model to a student model with the same size and architecture. GKD demonstrates its superior performance on self-distillation (Agarwal et al., 2024). We seek to evaluate whether \mathcal{X} -KD could surpass the performance of non-experiential KD approaches in self-distillation. To this end, we conducted comprehensive self-distillation experiments across the previously discussed three NLG tasks, implementing both G-XKD and GKD training objectives using the T5-large architecture. As illustrated in Table 3, G-XKD consistently demonstrates superior performance across all evaluation tasks. This consistent outperformance suggests that the experiential learning paradigm inherent in G-XKD offers substantial advantages even in scenarios where architectural differences between teacher and student models are eliminated.

B.3. Experiential Weight Ablation

The experiential weight λ in Equation 20 controls the degree of experiential learning since it scales the consistency between the policy and the reward function. In our primary experimental setup, we consistently maintained λ at 0.001 across all \mathcal{X} -KD methods. To comprehensively analyze the impact of the experiential weight, we conducted a systematic investigation by progressively increasing λ from 0.000 to 0.002, enabling us to observe the consequent effects on \mathcal{X} -KD performance metrics. Specifically, we implement SeqXD, S-XKD, and G-XKD under T5-large→T5-small setting with different λ configurations on the XSum dataset. As illustrated in Figure 3, as λ increases, the performance of all KD approaches shows a trend of first increasing and then decreasing, achieving the highest performance at $\lambda = 0.001$. This empirical observation underscores a notable limitation in our methodology, specifically its sensitivity to hyperparameter modifications. This susceptibility to parameter variation indicates that our training objective would benefit from additional normalization techniques.

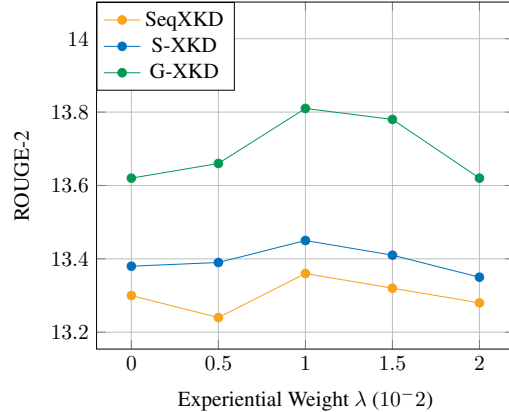


Figure 3. Performance under different experiential weights.

B.4. Boltzmann Temperature Ablation

The Boltzmann temperature τ' in Equation 28 controls the correlation between the Q value of each action and its probability under the LLM policy. A higher Boltzmann temperature indicates that the Q value is more affected by the action probability. In our primary experimental setup, we set τ' to 1.0 across all \mathcal{X} -KD methods. To evaluate the sensitivity of our framework to this crucial hyperparameter, we conducted a comprehensive ablation study by systematically varying τ' from 1.0 to 0.1. Like the experiential weight ablation, we implement SeqXD, S-XKD, and G-XKD under T5-large→T5-small setting with different τ' configurations on the XSum dataset. As demonstrated in Figure 4, all \mathcal{X} -KD methods achieve stable performances with respect to variations in the Boltzmann temperature and surpass the

corresponding non-experiential baselines (i.e., the dashed lines with corresponding colors.).

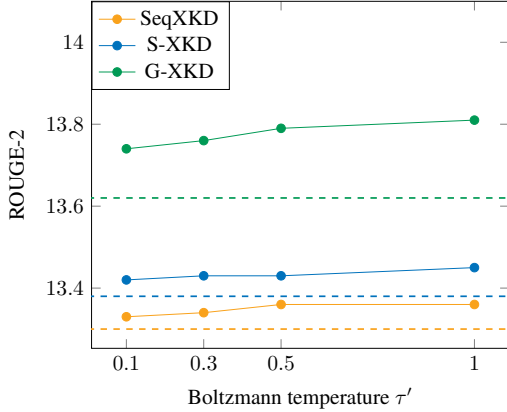


Figure 4. Performance under different Boltzmann temperature configurations. The dashed lines of different colors represent the performance of the corresponding non-experiential baselines.

C. Experiment Details

C.1. Supervised Fine-Tuning

Like GKD, we perform supervised fine-tuning for all student models and white-box teacher models on all three datasets.

Hardware. All SFTs are performed on 4 NVIDIA TITAN XP GPUs. For T5-small and T5-base, we use data parallel and fine-tune all parameters. For T5-large, we use model parallel and also fine-tune all parameters. For T5-xl, to save the GPU memory and speed up training, we adopt QLoRA (Dettmers et al., 2023), which quantizes the model in 8-bit and only fine-tunes the LoRA (Hu et al., 2021) adapters instead of all parameters.

Hyperparameters. Table 4 shows the SFT hyperparameters for T5-small and T5-base. For T5-large, we downscale the number of training steps by a factor of 0.4 and downscale the learning rate by factors of 0.05, 0.05, and 0.1 for three tasks respectively, as shown in Table 5. For T5-xl, we further downscale the training steps by factors of 1/8, 1/8, and 1/10 and downscale the learning rates by factors of 1/2, 1/2, and 1/3, as shown in Table 6. The batch sizes are also downscaled from 32 to 4.

C.2. Distillation to T5-small Student

Hardware. Distillation to T5-small student involves large→small in the primary setup and base→small and xl→small in the scalability study of additional experiments. For base→small and large→small, we simply use data parallel and perform training on 4 NVIDIA TITAN XP GPUs. For xl→small, for the teacher model (T5-xl), we use quantization and model parallel, and for the student model (T5-

small), we use data parallel. Note that in xl→small, we put the teacher model on 4 NVIDIA TITAN XP GPUs and put the student model on another 4 NVIDIA TITAN XP GPUs, which costs 8 GPUs in total. Since every 4 GPUs are on two different servers, we use Ray to build a cluster and ensure efficient communication.

Table 4. Hyperparameters for T5-small and T5-base SFT.

Hyperparameter	XSum	WMT	GSM8k
Training Steps	20k	100k	10k
Batch Size	32	32	32
Eval Split	validation	validation	test
Learning Rate (LR)	0.002	0.002	0.003
LR Schedule Type	linear	linear	linear
Warmup Steps	2k	2k	2k
Max Input Length	1024	64	512
Max Output Length	64	64	64

Table 5. Hyperparameters for T5-large SFT.

Hyperparameter	XSum	WMT	GSM8k
Training Steps	8k	40k	10k
Batch Size	32	32	32
Eval Split	validation	validation	test
Learning Rate (LR)	0.0001	0.0001	0.0003
LR Schedule Type	linear	linear	linear
Warmup Steps	2k	2k	2k
Max Input Length	1024	64	512
Max Output Length	64	64	64

Table 6. Hyperparameters for T5-xl SFT.

Hyperparameter	XSum	WMT	GSM8k
Training Steps	1k	5k	1k
Batch Size	4	4	4
Eval Split	validation	validation	test
Learning Rate (LR)	0.00005	0.00005	0.0001
LR Schedule Type	linear	linear	linear
Warmup Steps	0	0	0
Max Input Length	1024	64	512
Max Output Length	64	64	64

Hyperparameters. For three different model settings, we use the same hyperparameter configuration, as shown in Table 7. The *Sequence-Level* section contains the decoding hyperparameters for the teacher model. The general hyperparameters are identical to those in T5-small SFT (Table 4). Note that the batch size is only applied to gradient descent of the student model. The no-gradient forward through the teacher model uses a smaller batch size.

Table 7. Hyperparameters for distillations to T5-small and T5-base.

Hyperparameter	XSum	WMT	GSM8k
<i>General</i>			
Training Steps	20k	100k	10k
Batch Size	32	32	32
Eval Split	validation	validation	test
Learning Rate (LR)	0.002	0.002	0.001
LR Schedule Type	linear	linear	linear
Warmup Steps	2k	2k	2k
Max Input Length	1024	64	512
Max Output Length	64	64	64
<i>GKD</i>			
On-Policy Weight α	0.5	0.5	0.5
JS Divergence β	0.5	0.5	0.5
<i>Sequence-Level</i>			
Sampling Temperature	1.0	1.0	1.0
Top-p	0.95	0.95	0.95
<i>Experiential Learning</i>			
Discount Factor γ	1.0	1.0	1.0
Experiential Weight λ	0.001	0.001	0.001
Prior Distribution $p(R)$	Gaussian	Gaussian	Gaussian

C.3. Distillation to T5-base Student

Hardware. Distillation to T5-base student involves large \rightarrow base in the primary setup and xl \rightarrow base in the scalability study of additional experiments. For large \rightarrow base, we simply use data parallel and perform training on 4 NVIDIA TITAN XP GPUs. For xl \rightarrow base, we explicitly separate the teacher and the student, similar to xl \rightarrow small.

Hyperparameters. The hyperparameter configuration for distillation to T5-base is identical to that for distillation to T5-small, as shown in Table 7.

C.4. Distillation to T5-large Student

Hardware. Distillation to T5-large student involves black-box distillation from Llama-2-7b to T5-large in the primary setup and xl \rightarrow large in the scalability study of additional experiments. The black-box distillation consists of generating black-box teacher knowledge using Llama-2-7b and fine-tuning T5-large. We quantize Llama-2-7b with 4-bit quantization and put it on 4 NVIDIA TITAN XP GPUs while putting T5-large on another 4 NVIDIA TITAN XP GPUs with model parallel. For xl \rightarrow large, we also explicitly separate the teacher and the student, similar to xl \rightarrow small and xl \rightarrow base.

Hyperparameters. The hyperparameters for distillations to T5-large are shown in Table 8. The general hyperparameters are identical to those in T5-large SFT (Table 5). The decod-

ing hyperparameters in *Sequence-Level* section are applied to both black-box and white-box distillations.

Table 8. Hyperparameters for distillations to T5-large.

Hyperparameter	XSum	WMT	GSM8k
<i>General</i>			
Training Steps	8k	40k	10k
Batch Size	32	32	32
Eval Split	validation	validation	test
Learning Rate (LR)	0.0001	0.0001	0.0003
LR Schedule Type	linear	linear	linear
Warmup Steps	2k	2k	2k
Max Input Length	1024	64	512
Max Output Length	64	64	64
<i>GKD</i>			
On-Policy Weight α	0.5	0.5	0.5
JS Divergence β	0.5	0.5	0.5
<i>Sequence-Level</i>			
Sampling Temperature	1.0	1.0	1.0
Top-p	0.95	0.95	0.95
<i>Experiential Learning</i>			
Discount Factor γ	1.0	1.0	1.0
Experiential Weight λ	0.001	0.001	0.001
Prior Distribution $p(R)$	Gaussian	Gaussian	Gaussian